Atmospheric Environment 263 (2021) 118685

Contents lists available at ScienceDirect

Atmospheric Environment

journal homepage: www.elsevier.com/locate/atmosenv

Impact of the planetary boundary layer on air quality simulations over the Yangtze River Delta region, China

Lishu Shi [a,b], Ansheng Zhu [a,b], Ling Huang [a,b], Elly Yaluk [a,b], Ying Gu [c], Yangjun Wang [a,b], Shunyao Wang [a,b], Andy Chan [d,**], Li Li [a,b,*]

[a] School of Environmental and Chemical Engineering, Shanghai University, Shanghai 200444, China
[b] Key Laboratory of Organic Compound Pollution Control Engineering (MOE), Shanghai University, Shanghai 200444, China
[c] School of Air Transportation, Shanghai University of Engineering Science, Shanghai 201620, China
[d] Department of Civil Engineering, University of Nottingham Malaysia, Semenyih 43500, Selangor, Malaysia

HIGHLIGHTS

- Impacts from four PBL schemes within WRF on the simulation of air pollutants are evaluated over the YRD region.
- Seasonal and diurnal variations of surface pollutant concentrations are predicted and discussed.
- The MYNN scheme shows good performance for $PM_{2.5}$ and NO_2, while the YSU scheme is most suitable for O_3 prediction in the YRD.
- Implementing a single PBL scheme for a large area with complex topography is insufficient.

ARTICLE INFO

Keywords:
Planetary boundary layer
WRF-CAMx
Air quality simulation
Yangtze River Delta

ABSTRACT

The city clusters in eastern coastal China have suffered from serious air pollution in the past decades, which is partially related to the complex local topography and meteorological conditions. The planetary boundary layer (PBL) scheme is a critical parameter for accurate meteorology simulations and air quality predictions. In this study, we analyze the impact of four typical PBL schemes, namely, Yonsei University (YSU), Mellor-Yamada-Nakanishi-Niino Level 2.5 (MYNN), Asymmetric Convective Model version 2 (ACM2), and Mellor-Yamada-Janjic (MYJ) PBL, within the Weather Research and Forecasting (WRF) model to assess their impacts on the simulations of air pollutant concentrations based on the Comprehensive Air Quality Model with Extensions (CAMx) for the Yangtze River Delta (YRD) region, one of the most developed city clusters in eastern China. The results indicate that the MYNN scheme performs best in terms of fine particulate matter ($PM_{2.5}$) and nitrogen dioxide (NO_2) simulations, with mean bias of 4.8 μg m^{-3} and 9.3 μg m^{-3} in summer and 11.7 μg m^{-3} and 5.4 μg m^{-3} in winter, respectively. The YSU scheme performs best for ozone (O_3) prediction, with better simulation results in summer than in winter. Notably, some discrepancies among different PBL schemes in the prediction of air pollution are directly associated with the complex topography. For the prediction of $PM_{2.5}$, the MYJ and YSU schemes tend to overestimate the concentrations in the plains of Jiangsu and northern Anhui while underestimating $PM_{2.5}$ in the hilly areas compared with the MYNN scheme. Meanwhile, the performance of the ACM2 scheme is opposite to that of the MYJ and YSU schemes. For O_3 predictions, MYJ overestimates O_3 in the eastern coastal area and underestimates O_3 in the inland areas in summer compared with the YSU scheme, while the ACM2 scheme is the opposite of the MYJ scheme, and the MYNN scheme consistently overestimates O_3.

1. Introduction

Due to rapid industrialization and urbanization in recent decades, China has faced serious air pollution challenges (Chen et al., 2020; Fan et al., 2019). Surface air pollutant mixing ratios can be determined by various processes, such as emissions, transport and dispersion, chemical

* Corresponding author. School of Environmental and Chemical Engineering, Shanghai University, Shanghai 200444, China.
** Corresponding author.
E-mail addresses: Andy.Chan@nottingham.edu.my (A. Chan), Lily@shu.edu.cn (L. Li).

https://doi.org/10.1016/j.atmosenv.2021.118685
Received 2 May 2021; Received in revised form 12 August 2021; Accepted 13 August 2021
Available online 16 August 2021

transformation, and dry and wet deposition (He et al., 2018; Hu et al., 2015; Jiang et al., 2015; Zhai et al., 2019; Zu et al., 2017). These processes are typically dependent on meteorological conditions, which are greatly influenced by the planetary boundary layer (PBL) structures. Previous studies have indicated that $PM_{2.5}$ concentrations are negatively influenced by temperature (T), wind speed (WS), and the planetary boundary layer height (PBLH), and positively influenced by absolute humidity in most regions of China (Shi et al., 2020). The response of the ozone mixing ratio to temperature is a critical factor, and it is sensitive to the ozone formation mechanism or loss regime (Guicherit and Van Dop, 1977; He et al., 2018; Racherla and Adams, 2006). Therefore, the robustness of weather forecasts, typically using the WRF model, directly affects the performance of the subsequent air quality models (Storm and Basu, 2010; Zu et al., 2017). For instance, the exchange of moisture, heat, and momentum occurs within the PBL through mixing via turbulent eddies (Coniglio et al., 2013; Fountoukis et al., 2018), which can influence lower-tropospheric thermodynamics and kinematics (Holtslag and Moeng, 1964). Therefore, varying the selection of PBL schemes in the WRF model could have a significant influence on the simulated meteorological conditions and further affect the predictions of air pollution (André et al., 1978; Banks et al., 2016).

The PBL scheme includes both local and non-local closure schemes. For local closure schemes, only those vertical levels directly adjacent to a given site have a direct effect on the variables at a particular point (Ching et al., 2014). However, multiple vertical levels can be used to determine variables at a given point in non-local closure schemes (Stensrud, 2007). Previous studies have indicated that the simulation results under various PBL schemes for different types of pollutants in the same area could vary, while the performance also differs spatially and temporally (Chen et al., 2008; Li et al., 2020; Mao et al., 2006, 2006, 2006; Onwukwe and Jackson, 2020; Storm and Basu, 2010; Žabkar et al., 2013). Compared with simulations in a relatively large domain, PBL schemes are more sensitive to air quality in urban areas. A robust simulation of meteorological conditions is the foundation for accurate air quality modeling (Onwukwe and Jackson, 2020; Wang et al., 2015). Therefore, the choice of an appropriate boundary layer parameterization scheme has a significant influence on the simulation of the boundary layer structure, turbulence characteristics, and meteorological variables, which would further affect the performance of atmospheric modeling.

The YRD region is in the northern marine monsoon subtropical climate zone of southeast China, which is a well-developed city cluster. The topography of the YRD region is complicated, with mountains in the western and southern areas and adjacent to the ocean in the eastern region. In addition, the YRD region is in a transection area between the northern and southern parts of the country, with complicated meteorological conditions. Previous modeling studies have reported varying degrees of overestimation or underestimation of $PM_{2.5}$ and O_3 over the YRD region (Cheng et al., 2013; Fu et al., 2014; Huang et al., 2020; Li et al., 2018, 2020), which is partially associated with the bias of the meteorological parameters. Therefore, it is necessary to explore the influences of different boundary layer parameterization schemes on air quality predictions (including spatial and temporal differences) in the YRD region. In a parallel study , we assessed the results of four commonly used PBL schemes (YSU, ACM2, MYJ, and MYNN) to reproduce the meteorological variables in different seasons and evaluated their performance. In the current study, the main objective is to examine the impact of PBL schemes on regional air quality predictions. We evaluated the overall performance of the air quality model across monitoring stations and identified the most suitable PBL schemes for predicting air pollutants seasonally. The impact of PBL schemes on various terrains in the YRD region is also discussed. In addition, the seasonal and diurnal variations in air pollutants under the corresponding PBL schemes are also presented. This study evaluates the impacts of different PBL schemes in air quality models and discusses the appropriate parameter implementations, providing insights for further regional air quality simulations.

2. Methodology

2.1. Model configuration

An integrated modeling system comprising the Weather Research and Forecasting (WRF) model (version 4.0; https://www.mmm.ucar.edu/wrf-model-general) and the Comprehensive Air Quality Model with Extensions (CAMx) version 7.0 (http://www.camx.com/), was used to evaluate the role of PBL parameterization in air quality simulations. The gaseous and aerosol modules used in CAMx are the carbon bond (CB6) photochemical gas-phase mechanism (Yarwood et al., 2010) and the static two-mode coarse/fine (CF) PM chemistry option with ISORROPIA (Nenes et al., 1998). The aqueous-phase chemistry is based on the updated mechanism of the regional acid deposition model (RADM) (Chang et al., 1987). Three nested domains (Fig. 1.) are used where Domain 1 (D01) covers China, Japan, the Korean Peninsula, parts of India, and Southeast Asia with a grid spacing of 36 km; Domain 2 (D02) covers the eastern part of China with 12-km grid spacing and the inner domain (D03) covers the YRD region (Shanghai, Jiangsu, Zhejiang, Anhui provinces) and parts of surrounding areas with a grid spacing of 4 km $\times$ 4 km. The WRF meteorological modeling domain consists of three nested Lambert projection grids of 36, 12, and 4 km, with three grids larger than the CAMx modeling domain at each boundary. The WRF model is run simultaneously for the three nested domains with two-way feedback between the parent and nest grids, where all three domains utilize 39 vertical sigma layers, with the top layer at 50 hPa.

The initial and boundary conditions (IC/BCs) for the WRF modeling system are based on global final analysis (FNL) operational global analysis data with a $1^\circ \times 1^\circ$ grid archived at the Global Data Assimilation System. The BCs were updated at 6-h intervals for D01. In addition, the NOAH land surface scheme (Chen and Dudhia, 2001) was used to describe the land-atmosphere interactions, the Purdue-Lin microphysics scheme (Lin et al., 1983) was chosen to reproduce the cloud and precipitation processes, and the Rapid Radiative Transfer Model (RRTM) long-wave and Goddard Short-wave radiation schemes (Mlawer et al., 1997) were adopted to reflect the radiation.

In this study, anthropogenic emissions in China and other Asian regions were obtained from the 2017 Multi-resolution Emission Inventory of China (MEIC, http://www.meicmodel.org) developed by Tsinghua University and the 2010 Emissions Database for Global Atmospheric Research (EDGAR) emission inventory, respectively. The biogenic emissions were calculated using the updated Model of Emissions of Gases and Aerosols from Nature (MEGAN, v3.1, http://aqrp.ceer.utexas.edu/projects.cfm). Sea salt emissions were simulated using the OCEANIC pre-processor developed by Ramboll (http://www.camx.com/download/support-software.aspx), and the Sparse Matrix Operator Kernel Emissions (SMOKE, https://www.cmascenter.org/smoke) model was used to process emissions into the format required by the model. The simulation for the present study was based on summer (July) and winter (November) of 2018, and a five-day spin-up period was considered to mitigate the impact of the initial simulation conditions.

2.2. PBL parameterization

The PBL scheme is used to describe the vertical fluxes of heat, momentum, and moisture due to eddy transport within the entire atmospheric column in turbulent processes (Banks and Baldasano, 2016). One major component of the turbulence processes is whether a local or non-local mixing approach is employed. The local closure schemes obtain the turbulent fluxes using the mean variables and their gradients at each model grid, whereas the non-local closure schemes use multiple vertical levels and profiles of the convective boundary layer to determine the variables (Temimi et al., 2017). To date, 12 PBL schemes have been applied to the WRF model, and four of the most commonly used

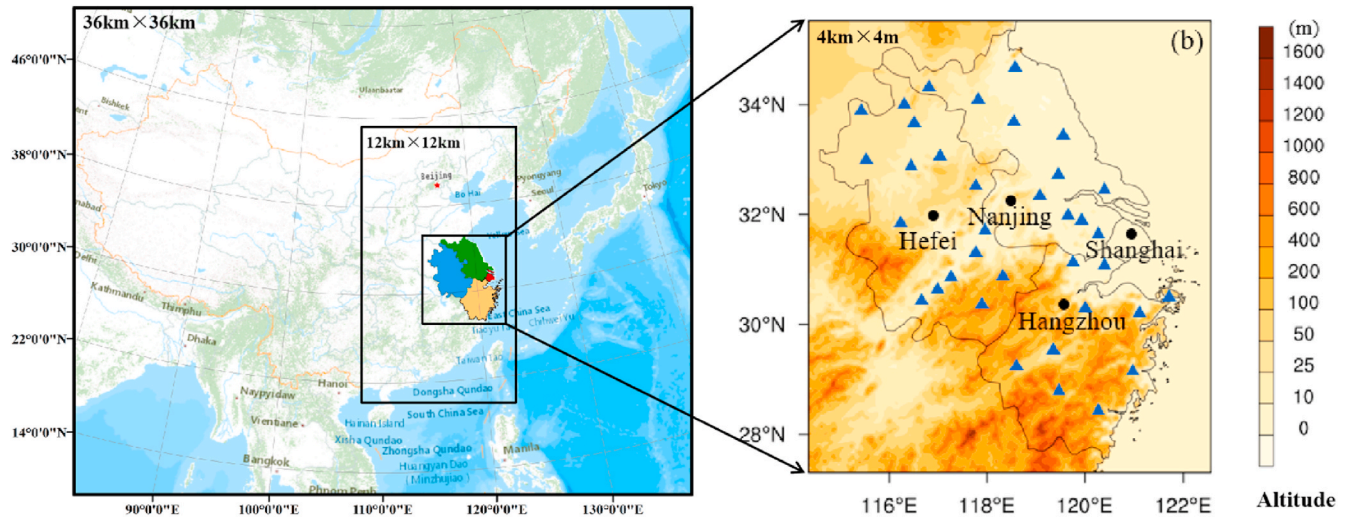

Fig. 1. Three nested modeling domain and locations of the national observational stations (blue triangle) and meteorological stations (dark dot). (For interpretation of the references to colour in this figure legend, the reader is referred to the Web version of this article.)

schemes (two local closure and two non-local closure schemes) have been selected to investigate their impacts on the air quality model performance in the current study (Table 1).

The YSU PBL scheme is a first-order non-local closure scheme. Revised from the Medium-Range Forecast (MRF) scheme, the significant improvement in YSU is the addition of an explicit term for the treatment of the entrainment process at the top (Jia and Zhang, 2020). Compared with MRF, the YSU scheme has more boundary layer mixing under thermally induced free convection conditions and less boundary layer mixing under mechanically induced forced convection conditions. The ACM2 scheme (Pleim, 2007) is a combination of ACM1, which adds an eddy diffusion component to the non-local transport. It calculates the PBL height using a critical bulk Richardson number of 0.25, similar to the YSU scheme. ACM2 was designed to better represent the shape of the vertical profiles, which could be more applicable to humidity, wind, or trace chemical mixing ratios in the boundary layer scheme. The MYJ scheme (Janjić and Zaviša, 1990) is a one-and-half-order local turbulence closure scheme. It diagnoses the vertical mixing process in PBL and free atmosphere by forecasting the TKE, combined with the additional prognostic equation of the TKE. The MYNN scheme is a one-and-half-order local closure scheme, which considers the effects of buoyancy on the diagnosis of the pressure covariance terms. It uses closure constants in the stability functions and mixing length formulations that are based on large eddy simulation results rather than observational datasets.

2.3. Observation data

The evaluation of meteorological prediction based on the WRF model and further study regarding the impact of various PBL schemes on meteorological simulation are presented in our companion study. In this work, we focus on the evaluation of air quality simulations using the CAMx model implemented with different PBL schemes.

To validate the air quality simulations, we used hourly surface observations of the major air pollutants (i.e., O_3, NO_2, SO_2, and $PM_{2.5}$) from the Ministry of Ecology and Environment of the People's Republic of China (http://datacenter.mep.gov.cn). As shown in Fig. 1, the pollution monitoring network over the YRD region consists of 41 monitoring stations distributed across 41 cities.

Statistical indices were applied to quantitatively assess the model performance, including the mean bias (MB), normalized mean bias (NMB), root-mean-square error (RMSE), fractional bias (FB), and index of agreement (IOA) (Huang et al., 2021). The equations for the selected indices for performance evaluation are listed in Table S1.

Table 1
Four PBL schemes evaluated in this study.

PBL scheme	Name	Closure	PBL height method
YSU	Yonsei University	non-local	Ri_b (bulk Richardson number) calculated from surface
MYNN	Mellor-Yamada-Nakanishi-Niino Level 2.5	local	turbulent kinetic energy (TKE)-prescribed threshold
ACM2	Asymmetric Convective Model version 2	Hybrid local-non-local	Ri_b calculated above neutral buoyancy level
MYJ	Mellor-Yamada-Janjic	local	TKE-prescribed threshold

3. Results and discussions

3.1. Evaluation of WRF meteorology

Meteorological variables from the WRF are significant drivers of CAMx air quality simulations. The 2-m air temperature (T2), 10-m wind speed (WS10), and relative humidity (RH) are critical variables for precise simulations. More details about the validation of meteorological variables can be found in our parallel work.

Tables S2 and S3 list the MB, RMSE, and R values for the WRF-simulated meteorological factors compared with the observations at the four airport stations in the YRD region. In brief, most of the PBL schemes underestimate the 2-m temperature in summer (−0.06–0.24 °C for July), while all four PBL schemes overestimate the 2-m temperature in winter (0.17–0.52 °C for November). All four PBL schemes overestimate 10-m WS (0.29–1.47 m/s for July; 0.25–0.66 m/s for November) but underestimate the RH (−4.0% to −5.86% for July; −5.86% to −11.03% for November). It should be noted that the overestimation of WS in summer was higher than that in winter. While the overall WRF works well for meteorology simulations, the performance of the four PBL schemes provides different indications.

3.2. Air quality evaluation

The predicted spatial distributions of the major air pollutants are shown in Fig. 2. In general, the monthly average concentrations of these air pollutants are consistent with the observations. The simulation

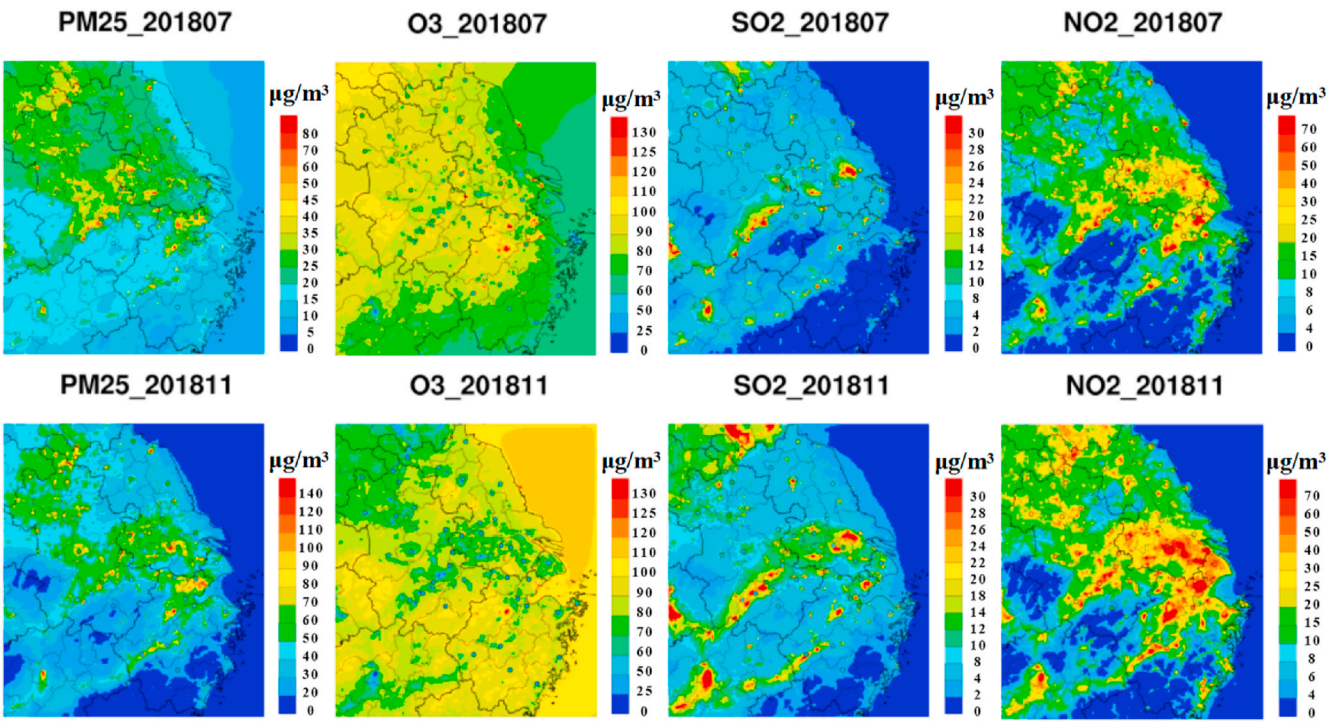

Fig. 2. Mean simulated (shaded) and observed (circles) concentrations of major air pollutants simulated by MYNN scheme in July and November 2018.

results in July are generally better than those in November. Specifically, the $PM_{2.5}$, SO_2, and NO_2 concentrations are higher in winter and lower in summer, but O_3 exhibits an opposite trend to that of $PM_{2.5}$. This is primarily due to the different meteorological conditions in summer and winter occurring in the monsoon zone. In addition, the observed $PM_{2.5}$ concentration generally demonstrates a decreasing trend from north to south of the YRD, while the O_3 concentration decreases from northwest to southeast in July, which was well captured by the model. The high concentrations of SO_2 and NO_2 are predominantly concentrated in the middle region of the YRD, and the simulation agreed well with the observations.

Fig. 3 presents the comprehensive statistical evaluation parameters between the observations and predictions of key pollutants at 41 national stations (corresponding to 41 cities) in the YRD region in July and November 2018. Based on the MB results, the performance of $PM_{2.5}$ and SO_2 simulation in July have better MB values of 4.8 μg m^{-3} and −0.4 μg m^{-3}, while O_3 and NO_2 are somewhat overestimated. However, all the pollutants except SO_2 were overestimated in November. Based on the IOA evaluation, O_3 is the highest, which is close to 0.7, followed by $PM_{2.5}$, and NO_2. Furthermore, our results demonstrate that the stations in Shanghai and Hangzhou have the best simulation of $PM_{2.5}$ and O_3 in July, with both the MB and NMB equal to zero (Table S4 and Table S5).

The model performances of the four PBL schemes differ from each other. The MYNN scheme achieved the best model simulation performance for $PM_{2.5}$, with an NMB of 20% in July, followed by SO_2 (NMB of 6%) and NO_2 (NMB of 59%), while the simulation results for O_3 (NMB of 33%) are the worst. Previous studies have clearly indicated that the local closure scheme is more suitable for the simulation of haze events (Li et al., 2016; Román-Cascón et al., 2012). Onwukwe and Jackson (2020) determined that the fully local MYJ and semi-local MYNN3 PBL schemes can more reasonably reproduce the peak-season concentrations of $PM_{2.5}$ and NO_2 than other schemes over a fjord valley. The second-order closure scheme (MYNN3) can more accurately portray deeper mixed layers compared with the MYNN scheme and reasonably depicts statically stable boundary layer simulations supporting radiation fog development (Nakanishi and Niino, 2006). Meanwhile, the MYNN scheme could improve the PBL depiction over non-local PBL schemes for springtime PBLs that support deep convection (Coniglio et al., 2013). The expressions of stability and mixing length by the MYNN scheme are based on the results of large eddy simulations rather than observations, while the expressions of mixing length are more applicable to a variety of static stability regimes (Mellor and Yamada, 1974, 1982). Therefore, the MYNN scheme is more likely to predict lower concentrations of near-surface air pollutants and perform better than non-local closure schemes under stable boundary layer conditions (Hu et al., 2013; Jia and Zhang, 2020).

Regarding the simulation of O_3, the YSU scheme performs better than MYNN, which is different from the results for $PM_{2.5}$. The O_3 mixing ratio has significant diurnal variations, with common peak concentrations observed in the afternoon. Furthermore, turbulence also normally reaches its peak between 12:00 and 14:00 (Yamada and Mellor, 1975) with the PBLH reaching its maximum. Therefore, O_3 is often affected by strong turbulence. However, the YSU scheme increases the buoyancy-driven vertical mixing and decreases the mechanically driven mixing, which alleviates the problems in the MRF scheme (Hong et al., 2005); therefore, it is more suitable for the simulation of pollutants under unstable conditions. Similarly, Cheng et al. (2012) also found that temperature, WS, and O_3 concentration simulated by the YSU scheme are closer to the observed daytime values, while the MYJ scheme is preferred at nighttime.

3.3. *Effect of meteorological variables and PBLH on air pollution prediction*

The PBL scheme affects the air quality simulation by influencing the meteorological parameters and boundary layer height derived from the WRF. Generally, the accumulation of pollutants is accompanied by higher RH, calm surface winds, low boundary layer height, and stronger anomalous temperature inversion within the PBL (John P. Dawson et al., 2007; J. P. Dawson et al., 2007; Shi et al., 2020). As shown in Figs. 4–7, the spatial differences in pollutant concentrations among the various schemes are primarily affected by the combination of meteorological parameters and the PBLH. However, our study did not analyze which parameter had the greatest impact on the difference in detail due to the

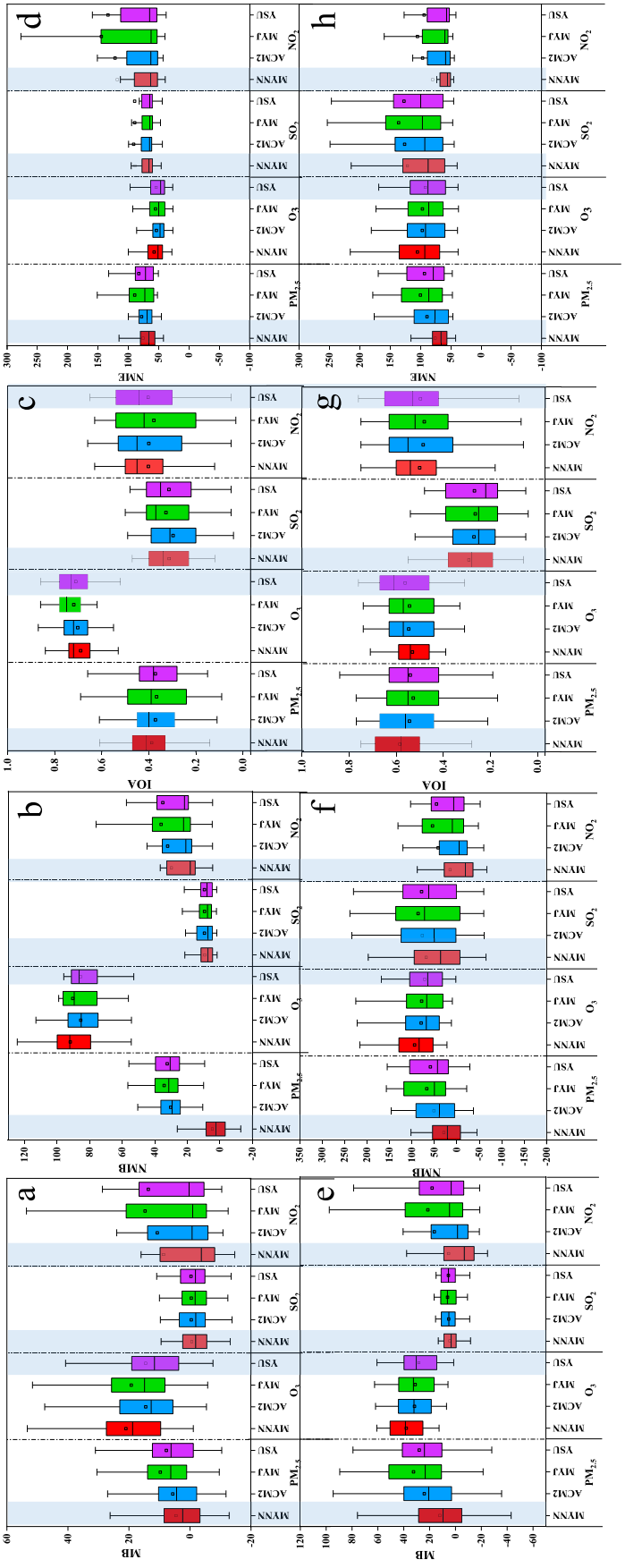

Fig. 3. Statistical model evaluation indices in 41 cities of the YRD region in July (a–d) and November (e–h) 2018.

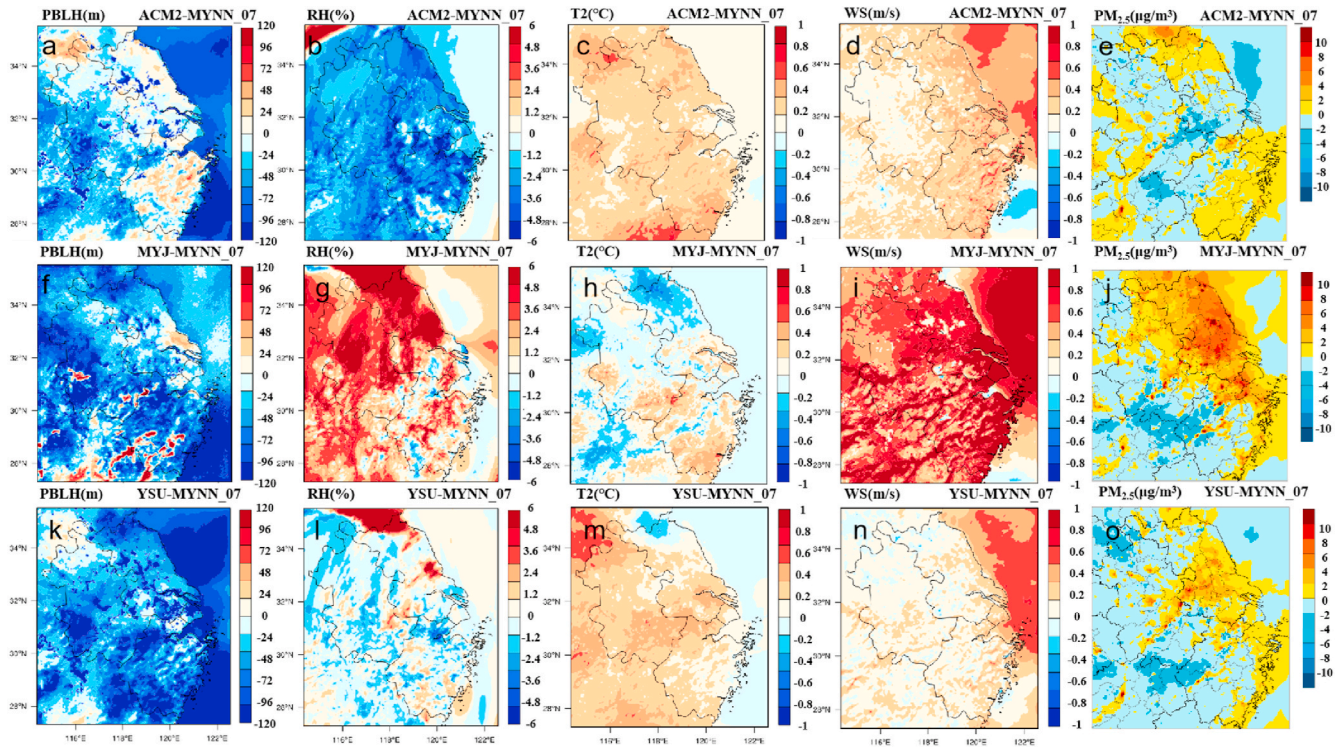

Fig. 4. Spatial bias of surface meteorological variables and pollutants, including RH, WS, T2, PBLH, and $PM_{2.5}$, in July. a–e display the bias between ACM2 and MYNN (ACM2-MYNN), f–j present the bias between MYJ and MYNN (MYJ-MYNN), and k–o show the bias between YSU and MYNN (YSU-MYNN).

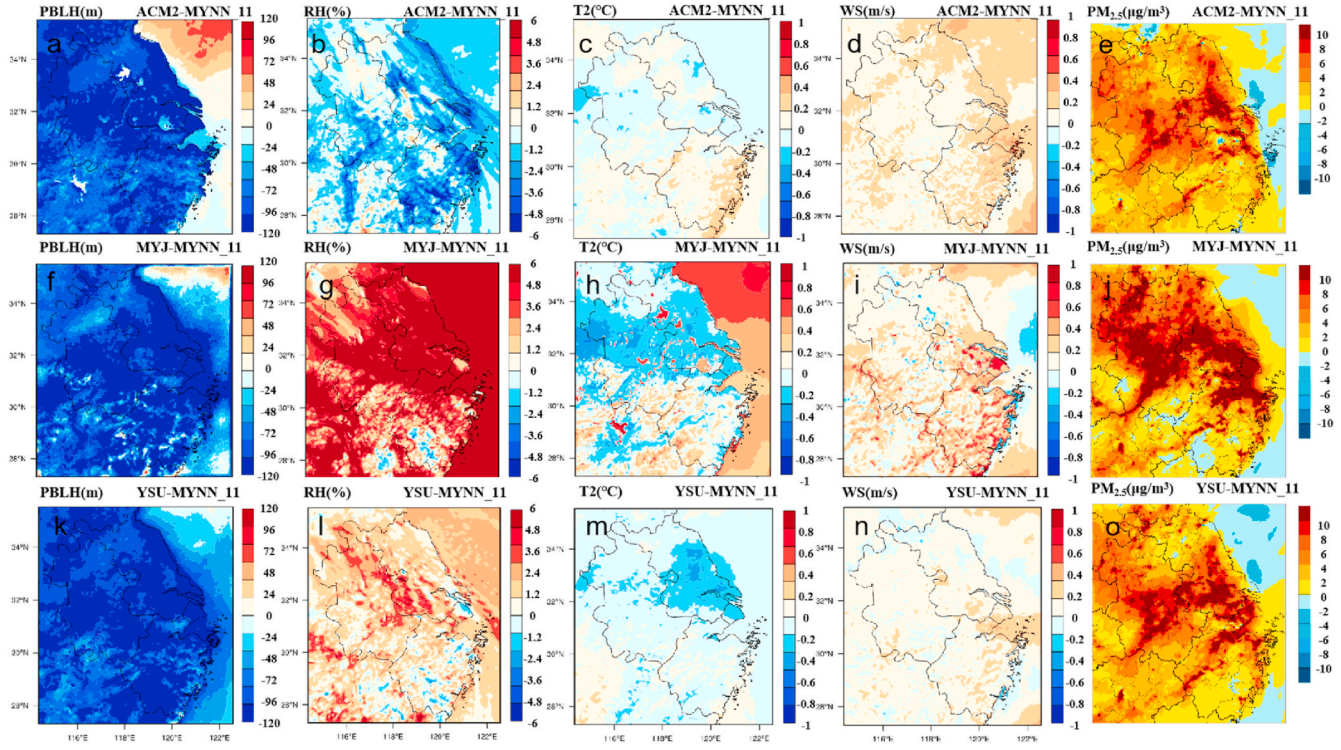

Fig. 5. Spatial bias of surface meteorological variables and pollutants, including RH, WS, T2, PBLH, and $PM_{2.5}$, in November. a–e demonstrate the bias between ACM2 and MYNN (ACM2-MYNN), f–j display the bias between MYJ and MYNN (MYJ-MYNN), and k–o present the bias between YSU and MYNN (YSU-MYNN).

complexity. In order to find the relationships between meteorological parameters and pollutants, we took the Shanghai station as an example (Fig. 8), finding that $PM_{2.5}$ and O_3 are positively correlated with temperature and negatively correlated with WS, while the influence of RH was weak. However, the potential effect of the PBLH on pollutant concentrations cannot be ignored.

In our parallel study, MYNN performed better for meteorological variables than the other three schemes in summer, while MYJ provides

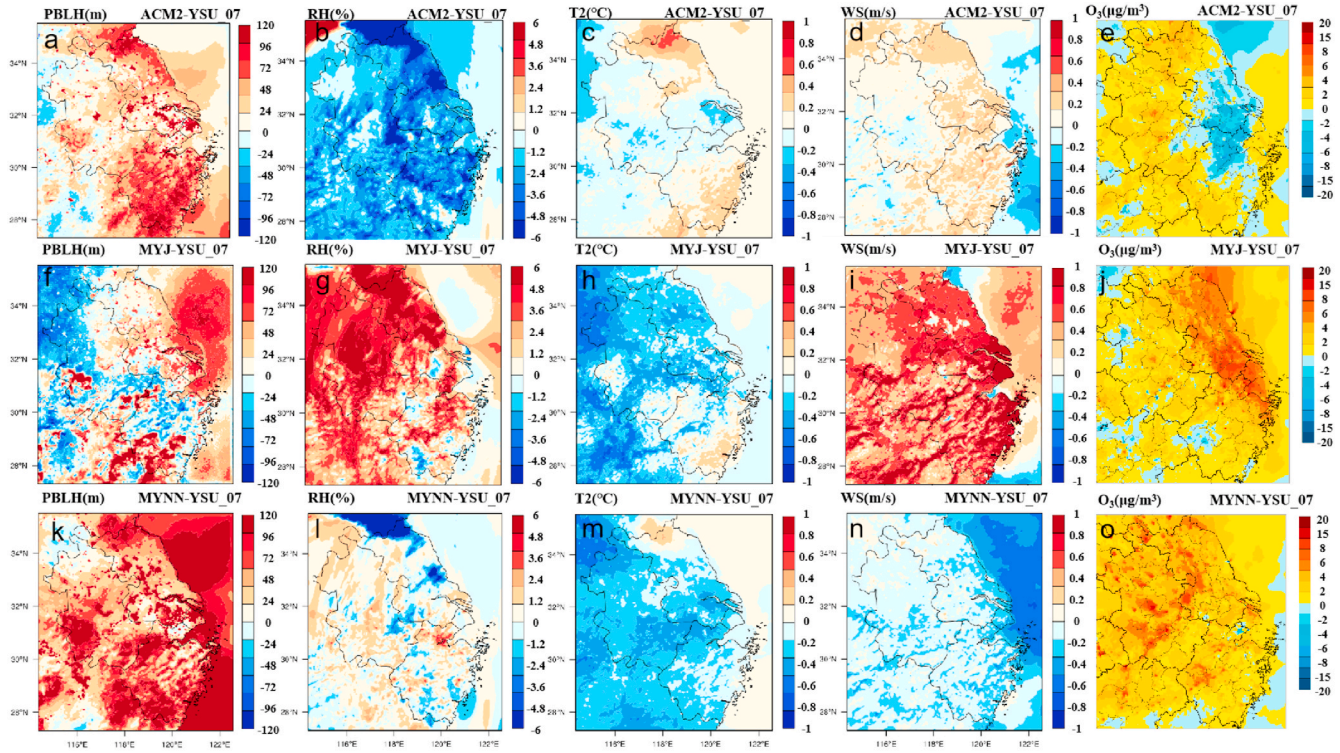

Fig. 6. Spatial bias of surface meteorological variables and pollutants, including RH, WS, T2, PBLH, and O_3, in July. a–e present the bias between ACM2 and MYNN (ACM2-MYNN), f–j display the bias between MYJ and MYNN (MYJ-MYNN), and k–o provide the bias between YSU and MYNN (YSU-MYNN).

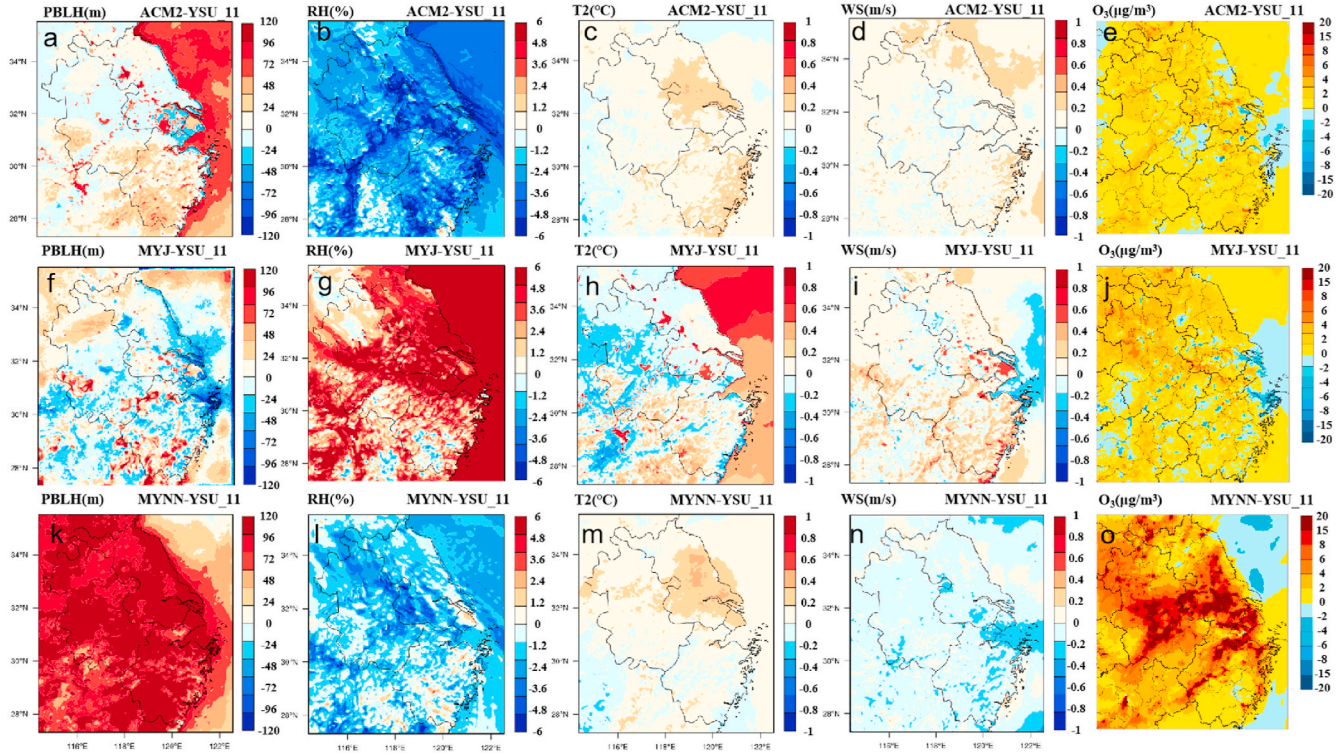

Fig. 7. Spatial bias of surface meteorological variables and pollutants including RH, WS, T2, PBLH, and O_3, in November. a–e show the bias between ACM2 and MYNN (ACM2-MYNN), f–j display the bias between MYJ and MYNN (MYJ-MYNN), and k–o illustrate the bias between YSU and MYNN (YSU-MYNN).

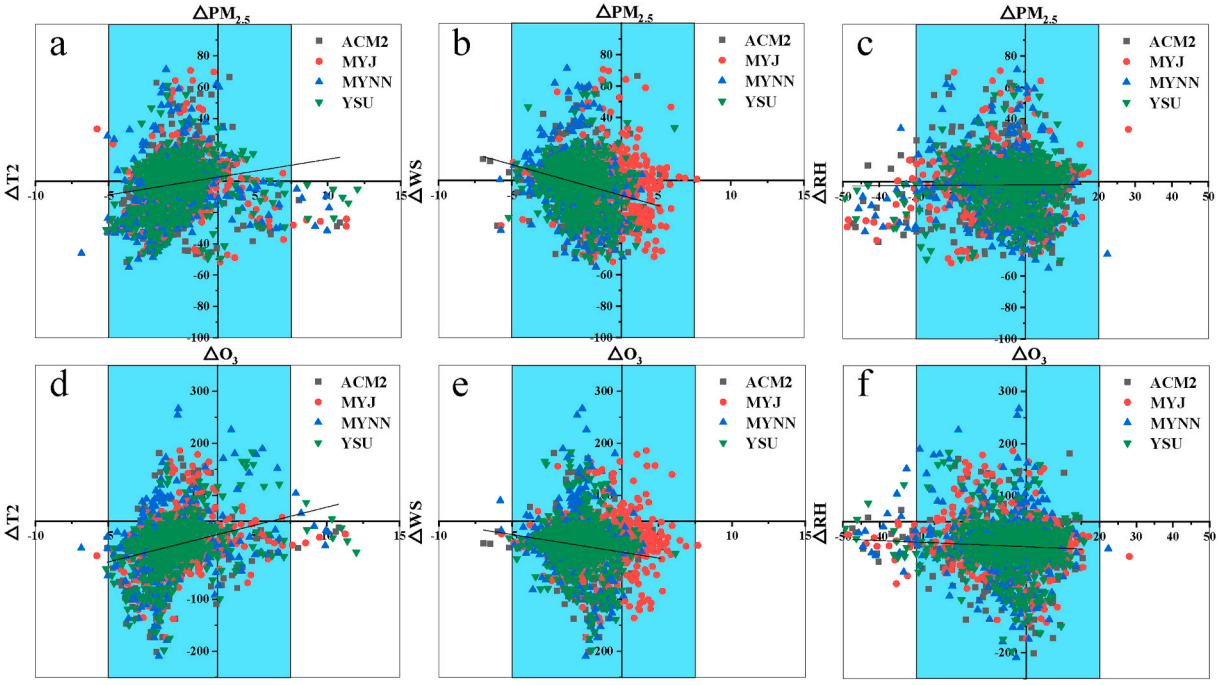

Fig. 8. Scatter diagrams of the relationship between the meteorological variable biases (△T2, △WS, △RH) and $PM_{2.5}$ and O_3 biases (PBL schemes – obs) at Shanghai station.

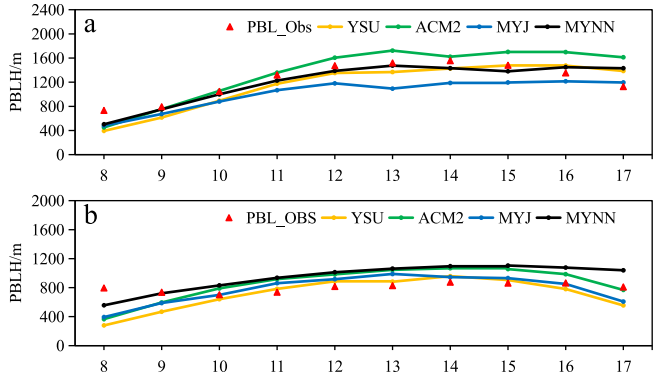

Fig. 9. Time series of daytime PBLH simulations and hourly average from lidar in July (a) and November (b).

better simulations in winter for the YRD region. Comparisons of the PBLH reveal that except for ACM2, the other three PBL schemes demonstrate various degrees of underestimation in summer (Fig. 9a). With the largest PBLH underestimation from the MYJ scheme and the best performance of the MYNN scheme, MYJ produced the largest overestimation of $PM_{2.5}$, while MYNN performed the best for $PM_{2.5}$ predictions. In November, the MYNN scheme simulated the highest PBLH (Fig. 5) but the lowest $PM_{2.5}$ concentration. Although the ACM2 scheme exhibits lower humidity and higher temperature/WS than the MYNN scheme, the predicted $PM_{2.5}$ concentration is still higher than that of the MYNN scheme. Therefore, the high deviation of PBLH has a great influence on the simulation of $PM_{2.5}$ compared with other meteorological variables. However, the O_3 results demonstrate characteristics that differ from those of $PM_{2.5}$. The YSU scheme exhibited the best simulation performance for O_3. Taking the YSU scheme as the benchmark, the O_3 concentration was overestimated when the PBLH was also overestimated, which may be because O_3 is affected by the PBLH, while temperature, WS, and boundary layer inversion also play a key role.

3.4. Diurnal variations driven by four PBL schemes

The diurnal variations of meteorological variables and pollutants in July and November with the four PBL schemes are presented in Fig. 10, which clearly shows how the PBL schemes can affect the simulation of the diurnal cycle of $PM_{2.5}$ and O_3. The peak $PM_{2.5}$ (Fig 10a, f) occurs in the morning due to the combined effects of traffic emissions during rush hour and a low PBLH. At noon, the $PM_{2.5}$ concentration drops mainly because of the highest boundary layer and the strongest vertical turbulent mixing. The simulation of diurnal $PM_{2.5}$ exhibited significant differences with the different PBL schemes, and the MYNN scheme performed better overall, especially for the meteorological variables (Fig. 10). In detail, the MYNN scheme provides a noticeable overestimation during the day in July and underestimation in November compared with the other schemes, which is primarily caused by the PBLH. Because the differences in the meteorological variables among the schemes are small, but the differences in boundary layer height are large (Fig. 9), the influence of the boundary layer height on pollutant concentration is greater than that of the meteorological variables. In general, the MYNN scheme performed better at night. The MYNN scheme is a local closure scheme, which is typically used to calculate mixing throughout the vertical extent of the model domain from the surface through the PBL and upwards to the top of the model.

Similarly, the diurnal O_3 trend simulated by each scheme was also investigated. (Fig 10b, g). The O_3 concentration reaches its peak in the afternoon, which is predominantly produced by photochemical reactions during the highest daily temperatures. In July, the simulation of

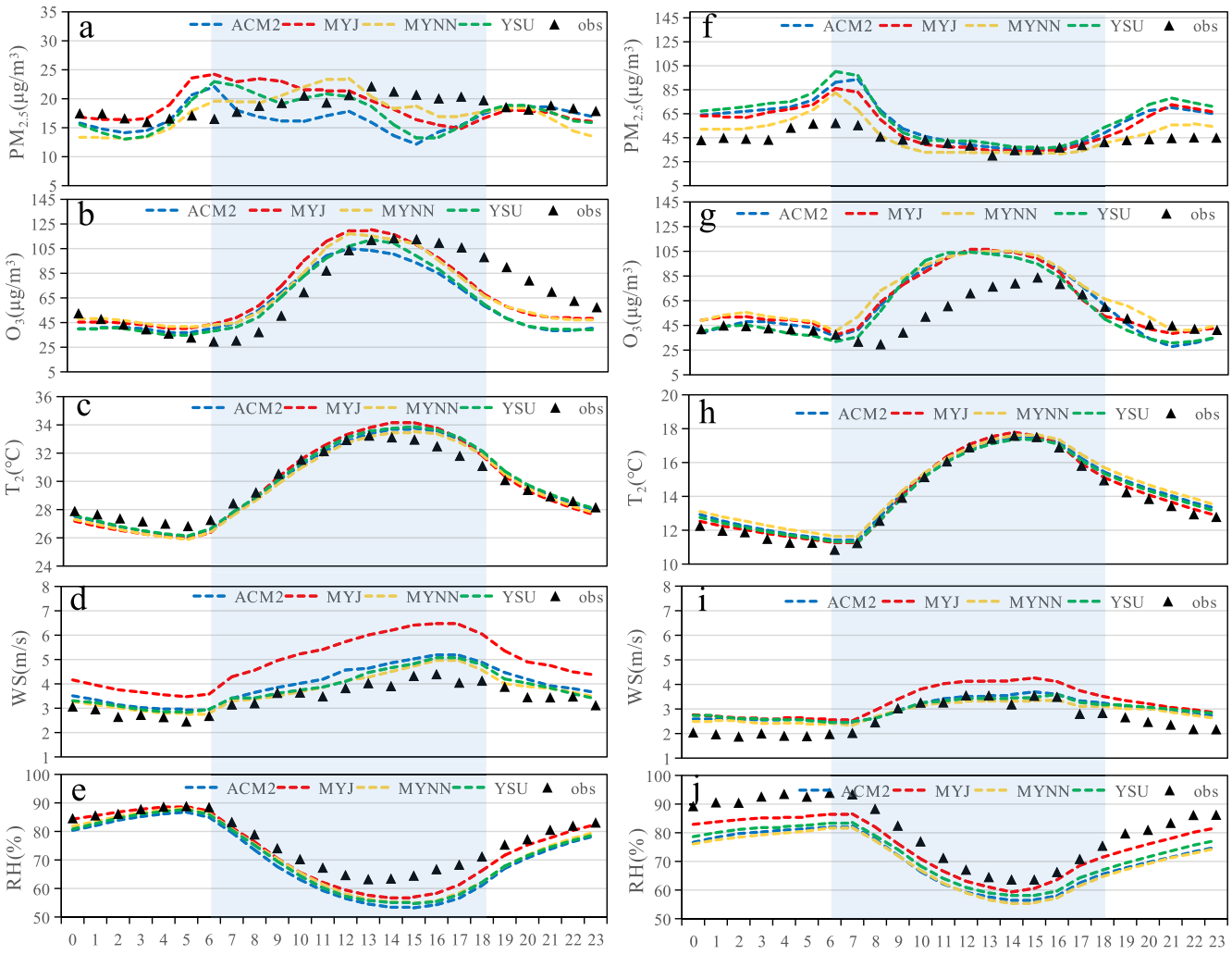

Fig. 10. Diurnal variations of the four PBL schemes for the meteorological variables (T2, WS, RH) and pollutants ($PM_{2.5}$, O_3) in the YRD region, including July (a–e) and November (f–j).

Table 2
Simulation differences of $PM_{2.5}$ (μg m^{-3}) and O_3 (μg m^{-3}) in different terrains of various PBL schemes in July and November. The Yangzhou, Yancheng, Jinhua and Huangshan stations represent plains, coastal/plains, hilly/coastal, and hilly, respectively.

		terrain	sim_MYNN	MB_MYNN	MYJ-MYNN	ACM2-MYNN	YSU-MYNN
$PM_{2.5}$	July	plains	52.55	−3.20	10.92	−4.16	2.74
		coastal/plains	17.57	5.10	4.60	−0.94	0.23
		hilly/coastal	29.07	7.40	−3.58	2.43	−1.62
		hilly	13.82	5.60	−0.97	−0.81	−0.41
	November	plains	114.66	−12.50	38.65	29.96	28.54
		coastal/plains	42.55	26.80	13.09	12.46	16.23
		hilly/coastal	65.98	31.90	8.55	6.13	8.41
		hilly	31.31	9.60	2.09	5.75	4.64
			sim_YSU	MB_YSU	MYJ-YSU	ACM2-YSU	MYNN-YSU
O_3	July	plains	120.93	10.20	10.98	−7.97	3.17
		coastal/plains	71.77	19.80	9.01	−1.52	9.20
		hilly/coastal	75.24	8.20	0.12	0.80	5.54
		hilly	83.28	0.00	0.38	1.60	2.10
	November	plains	84.61	1.40	1.30	2.06	8.25
		coastal/plains	78.98	31.80	3.87	4.33	13.72
		hilly/coastal	77.51	28.10	1.06	1.59	5.51
		hilly	85.53	10.20	2.44	0.65	5.79

O_3 in the daytime is typically overestimated and underestimated at night, while it mainly shows overestimation during the daytime in November. The simulation of O_3 by the MYNN and MYJ schemes usually showed the highest concentrations. In contrast, the O_3 concentration obtained by the YSU scheme was relatively low. There was little difference in the simulated diurnal variations among the different schemes.

3.5. Seasonal and spatial differences of the four PBL schemes

Based on the overall performance, the MYNN and YSU schemes were used as the basis for the $PM_{2.5}$, and O_3 analysis, respectively. First, we evaluated the spatial differences between the MYNN scheme (base) and the other PBL schemes for the prediction of the meteorological variables and $PM_{2.5}$ (Figs. 4 and 5, and Table 2).

The main topography of the YRD region can be characterized as the Zhejiang slopes in a stepped pattern from southwest to northeast, with mountains and hills dominating the southwest and middle regions, and a flat alluvial plain in the northeast (Fig. S3). Moreover, the topography of Anhui Province from north to south changes from plains to mountains. Jiangsu and Shanghai are relatively flat plains. We found that the PBL schemes exhibit different performances for different types of terrain. According to the bias error, the MYJ and YSU schemes mostly overestimate $PM_{2.5}$ in the plains of Jiangsu and northern part of Anhui, while underestimating the $PM_{2.5}$ level in the hilly areas of southern Anhui and Zhejiang, which are better than the July simulation results from the MYNN scheme. The ACM2 scheme primarily overestimates the concentrations in the coastal hilly region (Fig. 4 and Table 2). In winter, compared with the MYNN scheme, the other three schemes are all overestimated, which is likely due to the low transport capacity caused by the decrease in the PBLH and low turbulence during the cold weather in winter (Fig. 5). Similar to those in summer, the MYJ and YSU schemes also exhibited overestimation trends in the plains in winter. According to the spatial differences of the meteorological variables and pollutant types between the various schemes, the overestimation and underestimation of pollutants have no significant correlation with a particular variable, which is predominantly because the pollutant simulation is the result of interactions with the meteorological parameters, PBLH, and turbulence.

Similarly, the O_3 predictions were also analyzed (Figs. 6 and 7 and Table 2). The spatial difference in O_3 is quite different from that of $PM_{2.5}$. The ACM2 simulation typically performed better for O_3 in the plains of Jiangsu Province and coastal hilly region, while an overestimation is evident in the hilly areas of Anhui and Zhejiang in July (Fig. 6). Because the YSU scheme overestimates O_3 slightly, the ACM2 scheme has relatively good simulation results for the plains, but demonstrates a less precise prediction for the hilly area. The MYJ scheme overestimates O_3 in the eastern coastal area and underestimates it in the inland areas in summer, which is the opposite to that of the ACM2 scheme. Compared with the other three schemes, the MYNN scheme presented the worst performance in O_3 predictions.

Seasonally, the concentration of O_3 in winter is generally lower than that in summer because of the lower temperature and weak solar radiation. Our results indicate that O_3 in winter could be overestimated (Fig. 3). Overall, the simulation performance of the YSU scheme is the best, but it is still overestimated with a spatial difference of the bias similar to that predicted in summer. From these analyses, it can be concluded that an individual scheme has limited simulation ability for a large area with a complex topography. A modeling study is preferred for a relatively uniform topographic area to further improve the simulation accuracy of a PBL scheme. Otherwise, proper PBL schemes should be chosen considering the focused area, seasons, or pollutants. For large-scale area simulations, different PBL schemes can still reflect the variations in the simulation performance, and a relatively suitable PBL scheme can be recommended based on the evaluation results of the current study.

4. Conclusions

To explore the impacts of different PBL schemes on air quality simulations, four PBL schemes (YSU, MYJ, MYNN, and ACM2) were applied to the WRF-CAMx modeling system to predict the air quality in the YRD region. The results indicate that there are significant variations among the PBL schemes owing to mechanistic differences. From the overall simulation results of the YRD region, although there is little difference in the simulated concentrations among all the schemes, the most suitable scheme could still be identified. For instance, the MYNN scheme is most suitable for $PM_{2.5}$ and NO_2 predictions, while the YSU scheme has the best performance for O_3 predictions, and there is little difference in the SO_2 simulations among all the schemes for the months of July and November in the YRD. In terms of temporal variations, we found that large differences were predominantly reflected in the concentrations of pollutants, and there was no significant difference in the temporal variations produced by the four PBL schemes. Comparing the results from different seasons, the simulation performances from the schemes were more consistent over the YRD region, where the results for July are even better than those for November. The diurnal variation trends were consistent across all the schemes, where the differences in concentration among the schemes were smaller during the day than during the night. Regarding spatial differences, the PBL schemes demonstrated different performances in different terrains. The results indicate that the simulations of $PM_{2.5}$ by the MYJ and YSU schemes primarily overestimate the plain areas in Jiangsu and northern Anhui while producing better performances over the hilly areas in the southern part of Anhui and Zhejiang compared with the MYNN scheme. For the simulation of O_3, the ACM2 scheme typically performed better in the plains of Jiangsu Province and coastal hilly region while overestimating the hilly areas of Anhui and Zhejiang. Meanwhile, the results from the MYJ scheme demonstrated an opposite trend to that of the ACM2 scheme. The MYNN scheme is the worst for O_3 predictions compared with the other PBL schemes. From these analyses, it can be concluded that an individual scheme has a limited simulation ability for a large area with a complex topography. A modeling study is preferred for a relatively uniform topographic area to further improve the simulation accuracy of a PBL scheme.

CRediT authorship contribution statement

Lishu Shi: Formal analysis, Visualization, Writing. **Ansheng Zhu:** Formal analysis, Visualization, Writing. **Ling Huang:** Modeling, Visualization, Investigation. **Elly Yaluk:** Writing – review & editing. **Ying Gu:** Modeling, Visualization, Investigation. **Yangjun Wang:** Modeling, Visualization, Investigation. **Shunyao Wang:** Writing – review & editing. **Andy Chan:** Writing – review & editing. **Li Li:** Conceptualization, Methodology, Writing – review & editing.

Declaration of competing interest

The authors declare that they have no conflict of interest.

Acknowledgement

This study was financially supported by the National Natural Science Foundation of China (NO. 42075144, 41875161, 41105102), Shanghai International Science and Technology Cooperation Fund (No. 19230742500), the National Key R&D Program of China (No.2018YFC0213600), the Shanghai Science and Technology Innovation Plan (No.19DZ1205007), and the Shanghai Sail Program (No. 19YF1415600).

Appendix A. Supplementary data

Supplementary data to this article can be found online at https://doi.org/10.1016/j.atmosenv.2021.118685.

References

André, J.C., De Moor, G., Lacarrère, P., Du Vachat, R., 1978. Modeling the 24-hour evolution of the mean and turbulent structures of the planetary boundary layer. J. Atmos. Sci. 35 (10), 1861–1883.

Banks, R.F., Baldasano, J.M., 2016. Impact of WRF model PBL schemes on air quality simulations over Catalonia, Spain. Sci. Total Environ. 572, 98–113. https://doi.org/10.1016/j.scitotenv.2016.07.167.

Banks, Robert F., Tiana-Alsina, J., Maria Baldasano, J., Rocadenbosch, F., Papayannis, A., Solomos, S., Tzanis, C.G., 2016. Sensitivity of boundary-layer variables to PBL schemes in the WRF model based on surface meteorological observations, lidar, and radiosondes during the HygrA-CD campaign. Atmos. Res. 176–177 jul.-au), 185–201.

Chang, J.S., Brost, R.A., Isaksen, I.S.A., et al., 1987. A three-dimensional Eulerian acid deposition model: Physical concepts and formulation. J. Geophys. Res. Atmos. 92, 14681–14700. https://doi.org/10.1029/JD092iD12p14681.

Chen, F., Dudhia, J., 2001. Coupling an advanced land surface–hydrology model with the penn state–NCAR MM5 modeling system. Part I: model implementation and sensitivity. Mon. Weather Rev. 129 (4), 569–585.

Chen, J., Vaughan, J., Avise, J., O'Neill, S., Lamb, B., 2008. Enhancement and evaluation of the AIRPACT ozone and $PM_{2.5}$ forecast system for the Pacific Northwest. J. Geophys. Res. 113 (D14), D14305. https://doi.org/10.1029/2007JD009554.

Chen, C., Zhang, H., Li, H., Wu, N., Zhang, Q., 2020. Chemical characteristics and source apportionment of ambient $PM_{1.0}$ and $PM_{2.5}$ in a polluted city in North China plain. Atmos. Environ. 242, 117867. https://doi.org/10.1016/j.atmosenv.2020.117867.

Cheng, F.Y., Chin, S.C., Liu, T.H., 2012. The role of boundary layer schemes in meteorological and air quality simulations of the Taiwan area. Atmos. Environ. 54 (Jul), 714–727.

Cheng, Z., Wang, S., Jiang, J., Fu, Q., Chen, C., Xu, B., et al., 2013. Long-term trend of haze pollution and impact of particulate matter in the Yangtze River Delta, China. Environ. Pollut. 182, 101–110. https://doi.org/10.1016/j.envpol.2013.06.043.

Ching, J., Rotunno, R., Lemone, M., Martilli, A., Kosovic, B., Jimenez, P.A., Dudhia, J., 2014. Convectively induced secondary circulations in fine-grid mesoscale numerical weather prediction models. Mon. Weather Rev. 142 (9), 3284–3302.

Coniglio, M.C., Correia, J., Marsh, P.T., Kong, F., 2013. Verification of convection-allowing WRF model forecasts of the planetary boundary layer using sounding observations. Weather Forecast. 28 (3), 842–862.

Dawson, J.P., Adams, P.J., Pandis, S.N., 2007. Sensitivity of $PM_{2.5}$ to climate in the Eastern US: a modeling case study. Atmos. Chem. Phys. 7 (16).

Dawson, John P., Adams, P.J., Pandis, S.N., 2007. Sensitivity of ozone to summertime climate in the eastern USA: a modeling case study. Atmos. Environ. 41 (7), 1494–1511.

Fan, H., Zhao, C., Yang, Y., 2019. A Comprehensive Analysis of the Spatio-Temporal Variation of Urban Air Pollution in China during 2014-2018. Atmospheric Environment, p. 220.

Fountoukis, C., Ayoub, M.A., Ackermann, L., Perez-Astudillo, D., Bachour, D., Gladich, I., Hoehn, R.D., 2018. Vertical ozone concentration profiles in the arabian gulf region during summer and winter: sensitivity of WRF-chem to planetary boundary layer schemes. Aerosol and Air Quality Research 18 (5), 1183–1197. https://doi.org/10.4209/aaqr.2017.06.0194.

Fu, X., Wang, S.X., Cheng, Z., Xing, J., Zhao, B., Wang, J.D., Hao, J.M., 2014. Source, transport and impacts of a heavy dust event in the Yangtze River Delta, China, in 2011. Atmos. Chem. Phys. 14 (3), 1239–1254. https://doi.org/10.5194/acp-14-1239-2014.

Guicherit, R., Van Dop, H., 1977. Photochemical production of ozone in western Europe (1971-1975) and its relation to meteorology. Atmos. Environ. 11 (2), 145–155.

He, H., Liang, X.-Z., Wuebbles, D.J., 2018. Effects of emissions change, climate change and long-range transport on regional modeling of future U.S. particulate matter pollution and speciation. Atmos. Environ. 179, 166–176. https://doi.org/10.1016/j.atmosenv.2018.02.020.

Holtslag, A.A.M., Moeng, C.H., 1964. Eddy diffusivity and countergradient transport in the convective atmospheric boundary layer. J. Atmos. Sci. 48 (14), 1690–1700.

Hong, S.Y., Noh, Y., Dudhia, J., 2005. A new vertical diffusion package with an explicit treatment of entrainment processes. Mon. Weather Rev. 134 (9), 2318.

Hu, X.-M., Klein, P.M., Xue, M., 2013. Evaluation of the updated YSU planetary boundary layer scheme within WRF for wind resource and air quality assessments: impact OF vertical mixing ON wind and O_3. J. Geophys. Res.: Atmosphere 118 (18). https://doi.org/10.1002/jgrd.50823, 10,490-10,505.

Hu, J., Wu, L., Zheng, B., Zhang, Q., He, K., Chang, Q., et al., 2015. Source contributions and regional transport of primary particulate matter in China. Environ. Pollut. 207 (DEC), 31.

Huang, L., Wang, Q., Wang, Y., Emery, C., Zhu, A., Zhu, Y., et al., 2020. Simulation of Secondary Organic Aerosol over the Yangtze River Delta Region: the Impacts from the Emissions of Intermediate Volatility Organic Compounds and the SOA Modeling Framework. Atmospheric Environment. https://doi.org/10.1016/j.atmosenv.2020.118079, 118079.

Huang, L., Zhu, Y., Zhai, H., Xue, S., Zhu, T., Shao, Y., Liu, Z., Emery, C., Yarwood, G., Wang, Y., Fu, J., Zhang, K., Li, L., 2021. Recommendations on benchmarks for numerical air quality model applications in China – Part 1: $PM_{2.5}$ and chemical species. Atmos. Chem. Phys. 21, 2725–2743 https://doi.org/10.5194/acp-21-2725-2021.

Janji, ZaviA, I., 1990. The step-mountain coordinate: physical package. Mon. Weather Rev. 118 (7), 1429–1443.

Jia, W., Zhang, X., 2020. The role of the planetary boundary layer parameterization schemes on the meteorological and aerosol pollution simulations: a review. Atmos. Res. 239, 104890. https://doi.org/10.1016/j.atmosres.2020.104890.

Jiang, F., Ling, Z., Guo, H., et al., 2015. Simulation of ozone formation at different elevations in mountainous area of Hong Kong using WRF-CMAQ model. Sci. Total Environ. 505, 939–951. https://doi.org/10.1016/j.scitotenv.2014.10.070.

Li, L., An, J., Zhou, M., Qiao, L., Zhu, S., Yan, R., et al., 2018. An integrated source apportionment methodology and its application over the Yangtze River Delta region, China. Environ. Sci. Technol. 52, 14216–14227.

Li, R., Wang, Q., He, X., Zhu, S., Yu, J.Z., 2020. Source apportionment of $PM_{2.5}$ in Shanghai based on hourly organic molecular markers and other source tracers. Atmos. Chem. Phys. 20 (20), 12047–12061.

Li, T., Wang, H., Zhao, T., et al., 2016. The Impacts of Different PBL Schemes on the Simulation of PM $_{2.5}$ during Severe Haze Episodes in the Jing-Jin-Ji Region and Its Surroundings in China. Adv. Meteorol. 1–15. https://doi.org/10.1155/2016/6295878.

Lin, Y.L., Farley, R.D., Orville, H.D., 1983. Bulk parameterization of the snow field in a cloud model. J. Appl. Meteorol. 22 (6), 1065–1092.

Mao, Q., Gautney, L.L., Cook, T.M., Jacobs, M.E., Smith, S.N., Kelsoe, J.J., 2006. Numerical experiments on MM5–CMAQ sensitivity to various PBL schemes. Atmos. Environ. 40 (17), 3092–3110. https://doi.org/10.1016/j.atmosenv.2005.12.055.

Mellor, G.L., Yamada, T., 1974. A hierarchy of turbulence closure models for planetary boundary layers. J. Atmos. Sci. 31, 1791–1806.

Mellor, G.L., Yamada, T., 1982. Development of a turbulence closure model for geophysical fluid problems. Rev. Geophys. 20, 851–875.

Mlawer, E.J., Taubman, S.J., Brown, P.D., Iacono, M.J., Clough, S.A., 1997. Radiative transfer for inhomogeneous atmospheres: RRTM, a validated correlated-k model for the longwave. Journal of Geophysical Research Atmospheres 102 (D14).

Nakanishi, M., Niino, H., et al., 2006. An Improved Mellor–Yamada Level-3 Model: Its Numerical Stability and Application to a Regional Prediction of Advection Fog. Boundary-Layer Meteorol. 119, 397–407. https://doi.org/10.1007/s10546-005-9030-8.

Nenes, A., Pandis, S.N., Pilinis, C., 1998. ISORROPIA: a new thermodynamic equilibrium model for multiphase multicomponent inorganic aerosols. Aquat. Geochem. 4 (1), 123–152.

Onwukwe, C., Jackson, P.L., 2020. Evaluation of CMAQ modeling sensitivity to planetary boundary layer parameterizations for gaseous and particulate pollutants over a fjord valley. Atmos. Environ. 233, 117607. https://doi.org/10.1016/j.atmosenv.2020.117607.

Pleim, J.E., 2007. A combined local and nonlocal closure model for the atmospheric boundary layer. Part I: model description and testing. Journal of Applied Meteorology & Climatology 46 (9), 1383–1395.

Racherla, P.N., Adams, P.J., 2006. Sensitivity of global tropospheric ozone and fine particulate matter concentrations to climate change. J. Geophys. Res.: Atmosphere 111 (D24).

Román-Cascón, C., Yagüe, C., Sastre, M., Maqueda, G., Salamanca, F., Viana, S., 2012. Observations and WRF simulations of fog events at the Spanish Northern Plateau. Adv. Sci. Res. 8 (1), 11–18. https://doi.org/10.5194/asr-8-11-2012.

Shi, Z., Huang, L., Li, J., Ying, Q., Zhang, H., Hu, J., 2020. Sensitivity analysis of the surface ozone and fine particulate matter to meteorological parameters in China. Atmos. Chem. Phys. 20 (21), 13455–13466. https://doi.org/10.5194/acp-20-13455-2020.

Stensrud, D.J., 2007. Parametrization schemes. Keys to understanding numerical weather prediction models. Asian J. Res. Chem. https://doi.org/10.1017/CBO9780511812590.

Storm, B., Basu, S., 2010. The WRF model forecast-derived low-level wind shear climatology over the United States great plains. Energies 3 (2), 258–276. https://doi.org/10.3390/en3020258.

Temimi, Marouane, Weston, Michael, Chaouch, Naira, et al., 2017. Sensitivity of the meteorological model WRF-ARW to planetary boundary layer schemes during fog conditions in a coastal arid region. Atmos. Res. 106–127.

Wang, H., Xue, M., Zhang, X.Y., Liu, H.L., Zhou, C.H., Tan, S.C., et al., 2015. Mesoscale modeling study of the interactions between aerosols and PBL meteorology during a haze episode in Jing–Jin–Ji (China) and its nearby surrounding region – Part 1: aerosol distributions and meteorological features. Atmos. Chem. Phys. 15 (6), 3257–3275. https://doi.org/10.5194/acp-15-3257-2015.

Wang, N., Guo, H., Jiang, F., Ling, Z.H., Wang, T., 2015. Simulation of ozone formation at different elevations in mountainous area of Hong Kong using WRF-CMAQ model. Sci. Total Environ. 505, 939–951. https://doi.org/10.1016/j.scitotenv.2014.10.070.

Yamada, T., Mellor, G., 1975. A simulation of the wangara atmospheric boundary layer data. J. Atmos. Sci. 32 (12), 2309–2329.

Yarwood, G., Jung, J., Whitten, G.Z., et al., 2010. Updates to the Carbon Bond Mechanism for Version 6(CB6). Presented at the 9th Annual CMAS Conference, Chapel Hill, October.

Žabkar, R., Koračin, D., Rakovec, J., 2013. A WRF/Chem sensitivity study using ensemble modelling for a high ozone episode in Slovenia and the Northern Adriatic area. Atmos. Environ. 77, 990–1004. https://doi.org/10.1016/j.atmosenv.2013.05.065.

Zhai, S., Jacob, D.J., Wang, X., Shen, L., Li, K., Zhang, Y., et al., 2019. Fine particulate matter ($PM_{2.5}$) trends in China, 2013–2018: separating contributions from anthropogenic emissions and meteorology. Atmos. Chem. Phys. 19 (16), 11031–11041 https://doi.org/10.5194/acp-19-11031-2019.

Zu, Y., Huang, L., Hu, J., Zhao, Z., Liu, H., Zhang, H., et al., 2017. Investigation of relationships between meteorological conditions and high PM10 pollution in a megacity in the western Yangtze River Delta, China. Air Quality, Atmosphere & Health 10 (6), 713–724. https://doi.org/10.1007/s11869-017-0472-1.